Stem Cell Reports
Article

ISSCR

OPEN ACCESS

Ectopic recruitment of neuroblasts in striatal myelin bundles and nucleus accumbens following AraC chemical lesion

Irini Thanou,[1] Paraskevi N. Koutsoudaki,[2] Maria Margariti,[1] Federico Luzzati,[3] Sophia Havaki,[2] Vassilis G. Gorgoulis,[2,4,5,6,7] and Dimitra Thomaidou[1,8,*]

[1]Neural Stem Cells and Neuroimaging Group, Department of Neurobiology, Hellenic Pasteur Institute, 11521 Athens, Greece
[2]Molecular Carcinogenesis Group, Department of Histology and Embryology, Medical School, National and Kapodistrian University of Athens, 11527 Athens, Greece
[3]Department of Life Sciences and Systems Biology (DBIOS), University of Turin, Turin 10123, Italy Neuroscience Institute Cavalieri Ottolenghi (NICO), 10043 Orbassano, Italy
[4]Biomedical Research Foundation, Academy of Athens, Athens, Greece
[5]Ninewells Hospital and Medical School, University of Dundee, Dundee, UK
[6]Faculty Institute for Cancer Sciences, Manchester Academic Health Sciences Centre, University of Manchester, Manchester, UK
[7]Faculty of Health and Medical Sciences, University of Surrey, Guildford, UK
[8]Lead contact
*Correspondence: thomaidou@pasteur.gr
https://doi.org/10.1016/j.stemcr.2025.102636

SUMMARY

In the adult brain, neural stem cells (NSCs) constitutively generate new neurons in specific neurogenic domains. Recent research has unveiled reactive neurogenesis, whereby brain injury triggers NSC activation, enhancing their differentiation potential and guiding progeny to injured areas. Our study provides evidence of alternative migration pathways for newborn neurons in the mouse subcortical forebrain, revealed by administration of a chemotherapeutic agent. This allows a high number of newborn neurons to migrate long distances over an extended period. Notably, a subpopulation of neuroblasts diverts from the canonical SVZ-olfactory bulb (OB) rostral migratory stream toward the striatum (STR), with distinct localization along striatal myelin tracts and through nucleus accumbens (NAc) to the anterior commissure (AC). This neuroblast (NB) rerouting is accompanied by with oligodendrocyte lineage dysregulation and myelin deficits, suggesting a link between ectopic NB presence and observed myelin abnormalities.

INTRODUCTION

A wide range of pathological conditions, both neurodevelopmental and neurodegenerative, have been associated with defective or deficient neurogenesis. Conversely, during brain lesions/pathology, adult neurogenesis could serve as a pool for endogenous repair (Jin et al., 2001; Masuda et al., 2007). Some CNS injuries (e.g., stroke) stimulate neural stem cell (NSC) proliferation in canonical niches and induce ectopic migration of neuroblasts (NBs) (Arvidsson et al., 2002; Rice et al., 2003) and/or activation of local neural progenitor cells (Fogli et al., 2024; Magnusson et al., 2014; Nato et al., 2015). Thus, the subventricular zone (SVZ) represents a potential reservoir of precursor cells for brain repair (Grade and Götz, 2017).

Mounting evidence suggests that chemotherapeutic agents can lead to a form of brain chemical injury disrupting brain structure and function, collectively code-named "chemo brain," "chemo fog," or chemotherapy-induced cognitive impairment (CICI) (Nguyen and Ehrlich, 2020). Most chemotherapeutics function as cytostatics, aiming to reduce or halt the aberrant cell division of cancer cells. However, such a non-selectively inhibits all forms of cell division while it can also damage non-proliferating cells. Thus, neurogenic niches that are "hot spots" of physiological proliferation in the adult brain are particularly susceptible (Manda et al., 2014). Furthermore, chemotherapeutic treatments for CNS malignancies usually lead to a high concentration of chemotherapeutic agents in the cerebrospinal fluid (CSF) (Jacus et al., 2016; Wardill et al., 2016). This may further expose the SVZ neurogenic niche, which lies close to the lateral ventricle, to the effects of these chemicals. Therefore, a fundamental question arises: to what extent do the neurogenic niches in the adult brain respond to the impact of chemotherapeutic-induced chemical trauma and what does this imply for their regenerative capacity? While there is some data available, the majority of studies, often involving intracerebral infusion of mitotic inhibitors, have primarily focused on the structural aspects and lineage progression within these regions (Doetsch et al., 1999). To expand our understanding of how neurogenic niche of the SVZ and adjacent non-neurogenic regions respond to antimitotic agents, we conducted targeted intraventricular infusions of the commonly used chemotherapeutic antimitotic agent cytosine arabinoside (AraC) and assessed the different pathophysiological aspects of the imposed chemical damage on the SVZ and the surrounding brain parenchyma. Our findings indicate that AraC administration not only disrupts SVZ niche integrity and cytoarchitecture but also affects in neighboring dorsal and ventral striatal striatum (STR), with most prominent features being the recruitment of newborn NBs within

dorsal STR myelin bundles and nucleus accumbens (NAc) and the appearance of myelin defects in corpus callosum (CC) and STR white matter (WM).

RESULTS

Persistent disruption of SVZ niche integrity and ectopic recruitment of NBs in the STR and NAc

Our first goal was to evaluate SVZ niche response to AraC. To this end, we investigated the impact of AraC infusion on the ependymal layer and SVZ niche integrity, given the injection site's proximity to the ventricular walls. We assessed ependymal cell organization using the S100β marker following saline or AraC intraventricular infusion. To ensure the precision of our analysis, our measurements specifically concentrated on the ependymal layer, as S100β is also expressed in astroglial cells. Our data reveal a significant loss of the ependymal layer on the ipsilateral side, a condition evident as early as 4 days and persisting up to 6 weeks after AraC infusion (Figures 1A and 1C). At the same time, qualitative analysis of CD133 (prominin-1), expressed by multiciliated ependymal cells and the primary cilium of NSCs, indicates substantial loss of the ependymal cell population (Figure 1A). In parallel, GFAP immunostaining reveals a loss of the astrocyte layer and instead accumulation of hypertrophic astrocytes in the SVZ and neighboring parenchyma (Figure 1B), consistent with previous findings that loss of ependymal layer and niche progenitors triggers astrocytes to form a glial scar to replenish the lost barrier (Luo et al., 2008). Collectively, these data indicate a prolonged and extensive denudation of the ependymal barrier in our model, partially substituted by astroglial scar formation.

To further assess the impact of AraC on the SVZ niche dynamics, we examined the fast-proliferating progenitors, known as transit-amplifying cells. Utilizing the Ki67 proliferation marker, we observed a notable reduction in proliferating niche cells, as expected, at 15-day and 6-week time points post-infusion (p.i.) (Figures 1D and 1F). This decline occurred bilateral but more pronounced on the ipsilateral side when compared to the contralateral side (Figures 1D–1F and 1G). Consistent with an intact ependymal layer, the saline-treated group showed no significant difference in SVZ proliferation (Figure 1F). Interestingly, we also observed the significant decrease in MASH1 (ASCL1) progenitors on the ipsilateral side at the 6-week time point, but not contralaterally (Figures 1E and 1H), suggesting that although proliferation is affected throughout the SVZ niche, a subset of progenitors is preserved in the, more distant to the chemical insult, contralateral side. Overall, these data suggest that compensatory mechanisms may occur on the contralaterally, which cannot be activated to the same extent on the more severely affected ipsilateral side.

Furthermore, while the population of DCX$^+$ NBs located in the lateral walls showed a marked reduction compared to normal conditions (Figures 1D and 1E), there is a marked increase of DCX$^+$ cell numbers in the STR, which is accompanied by a more dispersed pattern of their localization around the rostral migratory stream (Figures 2A and S1A). Additionally, a subpopulation of DCX$^+$ NBs is localized in brain parenchyma regions adjacent to the SVZ niche (Figure 2A). In particular, both chains of DCX$^+$ NBs (circled) and single migrating NBs are observed in the STR (Figure 2B, yellow arrow), in the CC, and to a lesser extent, in the cortex and septum (Figure 2A). Notably, striatal accumulation of NBs increases with time and is much more pronounced ipsilaterally, than contralaterally (Figure 2C). An intriguing observation was that AraC insult also induces a ventral SVZ response toward the NAc (Figure 2A). As previously reported, a dense cluster of NBs is normally observed in the ventral SVZ (Sundholm-Peters et al., 2004), reported to give rise to medium spiny neurons (MSNs) in the NAc during adulthood (García-González et al., 2021). In our model, this cluster appears dispersed accompanied by migration of DCX$^+$ NBs, mainly toward the NAc, and the AC (Figure 2A). Spatial mapping of DCX$^+$ NB localization adjacent to the SVZ along the dorsoventral axis 6 weeks following AraC revealed the presence of at least three exit points of NBs from the SVZ: one in the lateral SVZ-RMS axis (Figure 2E), one in the lateral SVZ (Figure 2E′) and a later in the ventral SVZ (Figure 2E″). As expected, this diversion disrupts the RMS, resulting in fewer NBs reaching the olfactory bulb (OB) and aberrant migration patterns among those that do (Figures S1B–S1E). This indicates an overall reduction in adult neurogenesis within the OB.

Migratory ectopic NBs accumulate in striatal myelin bundles or differentiate when lying in gray matter

We next analyzed the ectopic recruitment of DCX$^+$ NBs in the STR, as it the area with highest cell accumulation. Co-staining with the myelin marker CNPase revealed that DCX$^+$ migratory NBs are mainly located along the myelin tracts of dorso-medial and ventro-medial quadrants of the STR (Figures 3A–3C) and migrating rostrocaudally along the internal capsule (IC) (Figures 3B and 3C). Quantification of DCX$^+$ ectopic cells in the STR confirms that the majority of them are found within myelin bundles (Figures 3D and 3E). The rerouting of a subpopulation of NBs to the striatal myelin tracks, from their default SVZ-RMS migration route, does not initiate acutely, as only few NBs are localized in the STR 4 days p.i. Numerous redirected DCX$^+$ NBs become evident ipsilaterally 15 days p.i. and their number increases at 6 weeks (Figures 2C, 2D, 3D, and 3E).

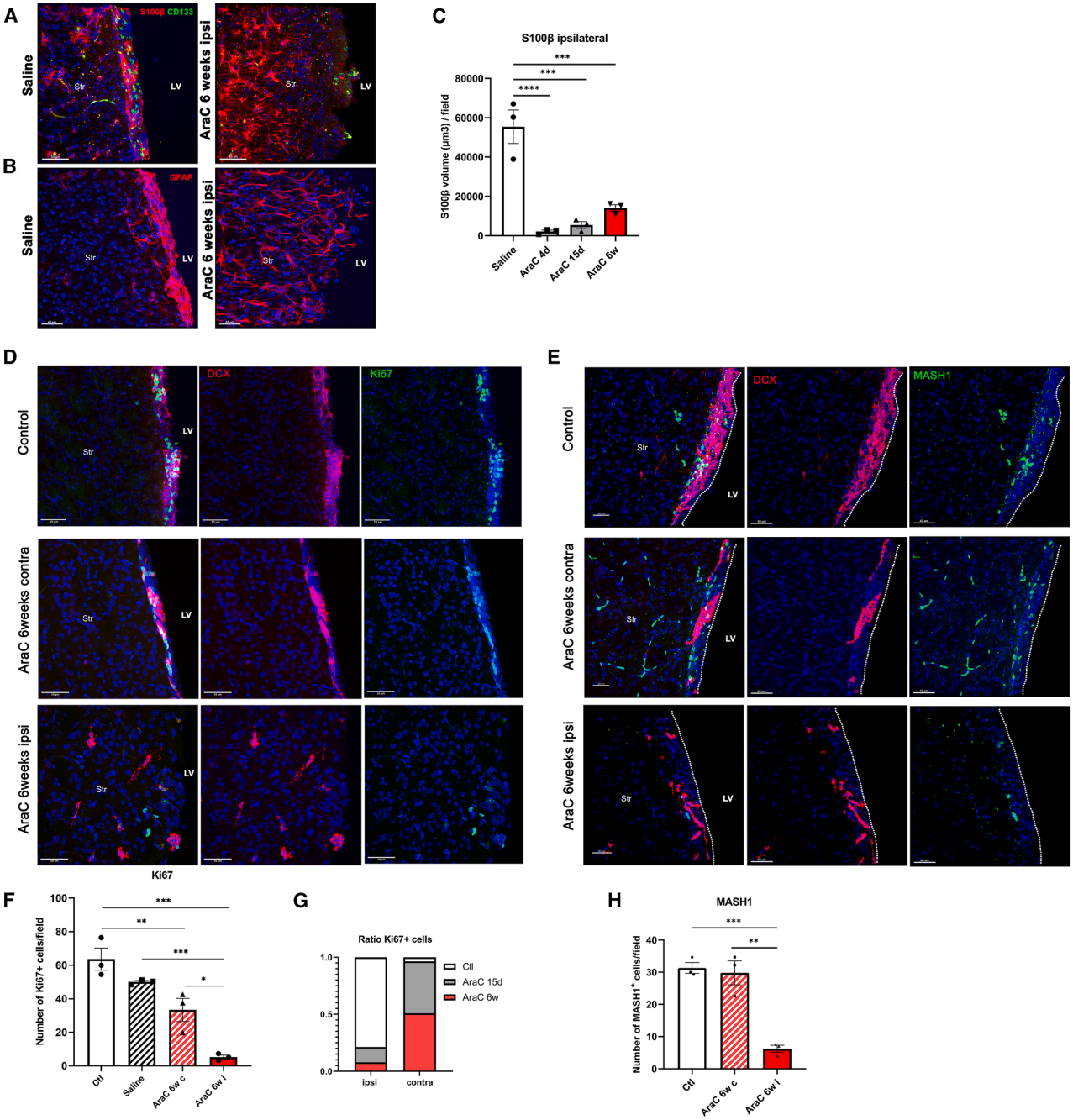

Figure 1. SVZ niche integrity disruption

(A and B) IHC representative images of (A) S100β and CD133 (B) GFAP in lateral wall.

(C–E) (C) IHC quantification of S100β volume for the ipsilateral SVZ wall. IHC representative images of (D) DCX and Ki67 (E) DCX and MASH1, ipsi and contra to the infusion side.

(F) IHC quantification of $Ki67^+$ cells in lateral SVZ per field.

(G) Ratio of $Ki67^+$ cells in AraC-treated groups (15 days and 6 weeks) normalized to Ctl. Gray and red bars show percent decline relative to Ctl (white).

(H) IHC quantification of $MASH1^+$ cells in lateral SVZ per field (vascular labeling is likely cross-reactivity).

Dots in graphs (C, F, and H) represent different mice. Animals: $n = 3$ (male and female). Data represent mean ± SEM. $^*p \leq 0.05$, $^{**}p \leq 0.01$, and $^{***}p \leq 0.001$ (one-way ANOVA). Scale bars: (A and D) 50 µm, (B) 40 µm, and (E) 30 µm.

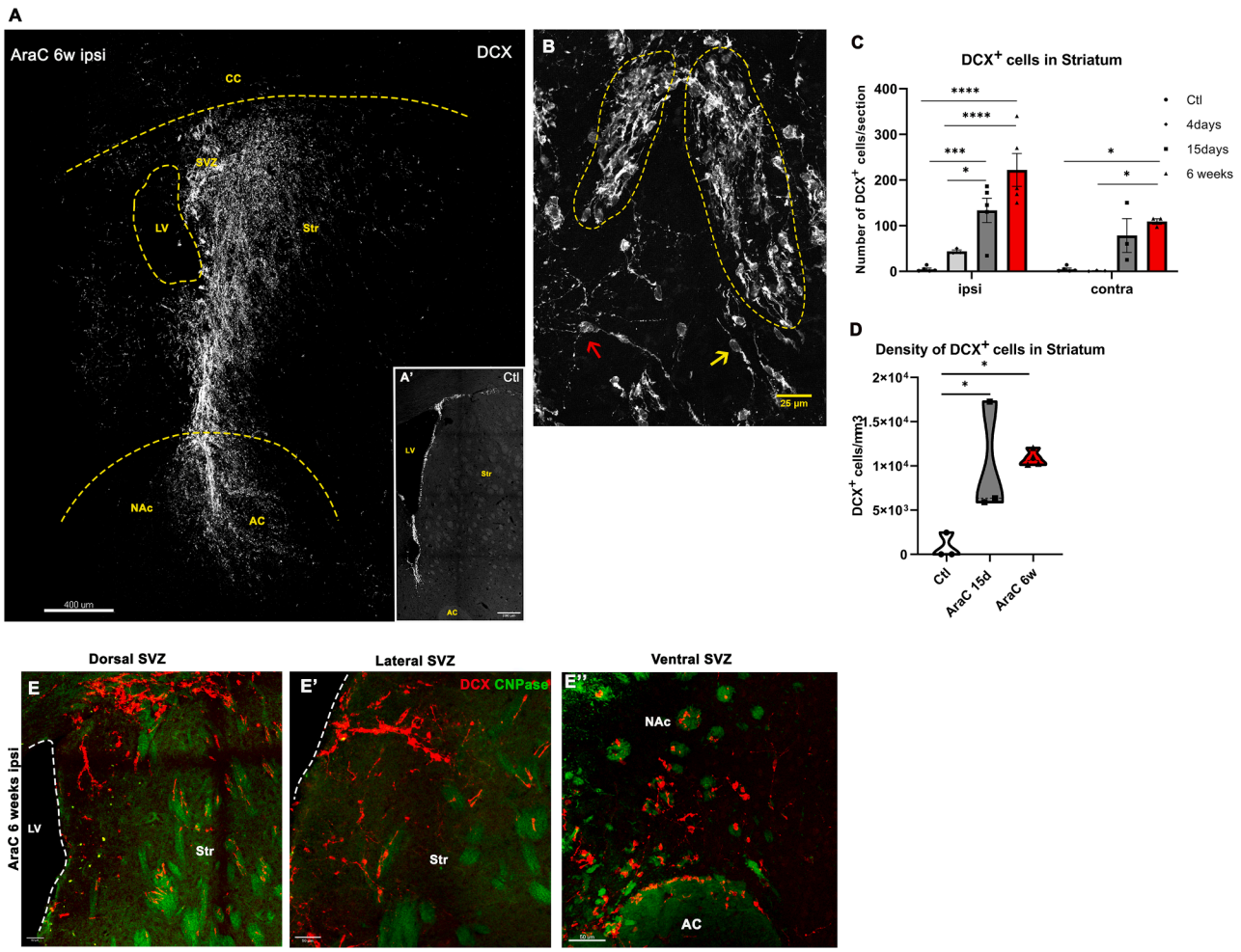

Figure 2. Ectopic recruitment of NBs to STR and NAc toward AC

(A) 3D reconstruction of DCX$^+$ NBs ectopic distribution to STR and NAc 6 weeks p.i. (see also Methods S1). (A′) DCX$^+$ NBs distribution (gray) in Ctl SVZ. No ectopic DCX observed.

(B) Higher-magnification 3D reconstruction showing NB clusters within myelin tracts (yellow dashed outline) of the STR, individual migratory bipolar cells (yellow arrow), and more mature neuronal phenotypes (red arrow).

(C) Quantification of ectopic DCX+ cells in the STR per section.

(D) Density of DCX$^+$ cells in the ipsi STR. Confocal images of DCX and CNPase at exit sites from the SVZ to adjacent parenchymal areas.

(E) Chains of NBs leaving the RMS and entering myelin tracts.

(E′) Chains and single NBs detaching from the lateral SVZ wall.

(E″) NBs from the ventral SVZ entering the anterior commissure (AC).

Dots in (C and D) represent different mice. Animals: $n = 3–4$ (male and female). Data represent mean ± SEM. *$p \leq 0.05$, ***$p \leq 0.001$, and ****$p \leq 0.0001$ (one-way ANOVA). Scale bars: (A) 400 µm, (A′) 200 µm, (B) 25 µm, and (E–E″) 50 µm.

To confirm that myelin bundles serve as the migrating substrate of redirected NBs and to assess the magnitude of migrating cells, we performed 3D reconstruction of tracts and cells along them 6 weeks p.i. We observed that throughout the bundles, chains of migrating NBs are densely clustered and appear to follow the anteroposterior and dorsoventral direction of the myelin bundles (Figure 3F). Additional immunohistochemical staining showing presence of DCX$^+$ cells in epoxy semi-thin brain sections (Figure 3G) confirmed our prior findings. Moreover, electron microscopy (EM) analysis demonstrated that numerous NBs located along myelin tracts contain quite a few autophagosomes (Figure 3H, arrow) indicating their migratory phase (Bressan et al., 2020).

We further characterized the DCX$^+$ ectopic cells, mainly organized in chains along myelin fibers (Figures 2B, 3F and 4A), to gain a better insight into their identity. Immunofluorescence experiments show no colocalization of

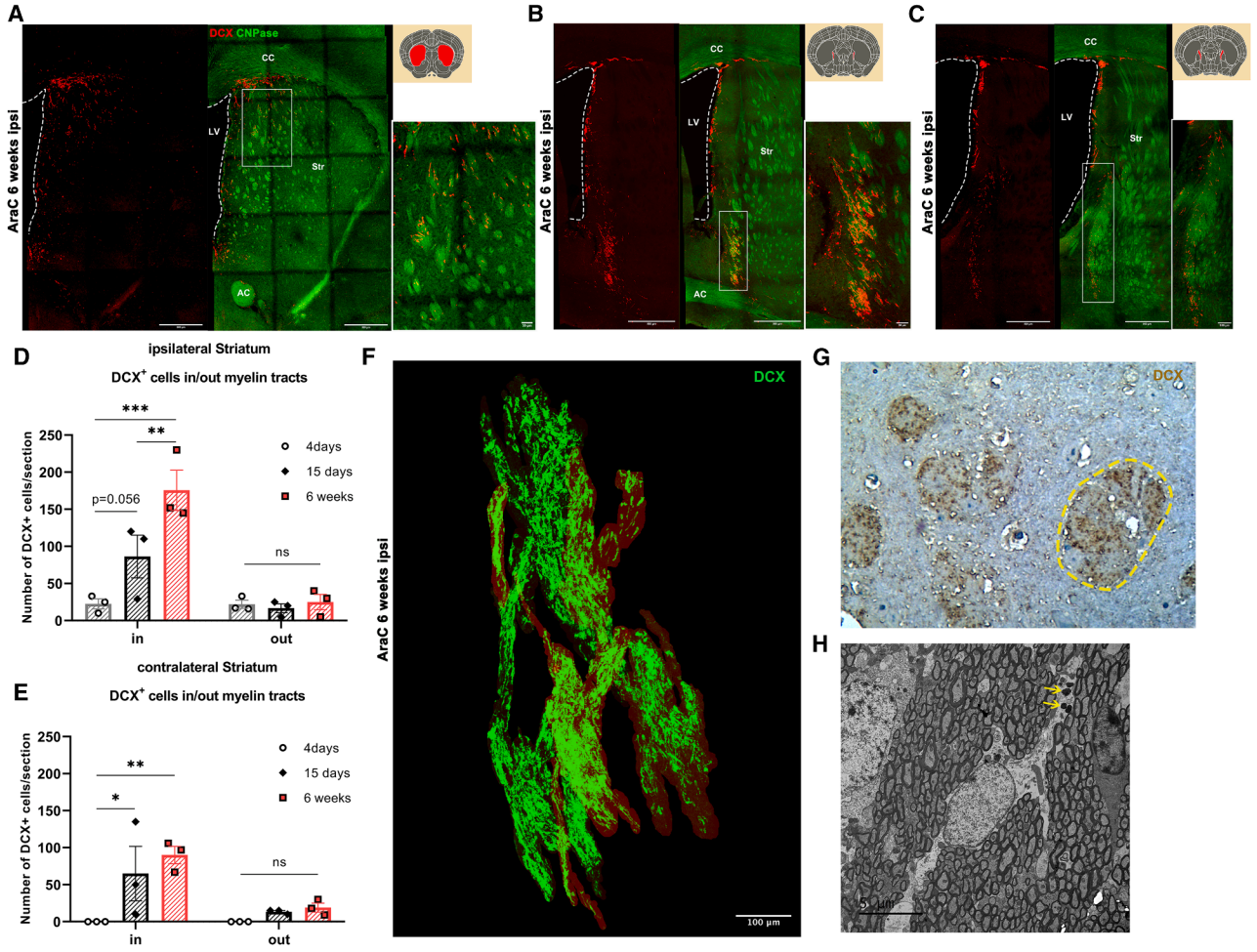

Figure 3. NBs accumulation along striatal myelin bundles

(A–C) Representative images of ectopic DCX$^+$ cell distribution along the anterior-posterior ipsilateral STR in AraC, 6 weeks. Most NBs (DCX, red) localize in myelin tracts (CNPase, green). Insets (Scalable Brain Atlas) show highlighted brain regions (A: caudoputamen; B and C: internal capsule).

(D and E) Quantification of ectopic DCX$^+$ cells inside and outside striatal myelin bundles ipsi (D) and contra (E) to the infusion site.

(F) 3D reconstruction of myelin bundles (masked neurofilament, red) and NBs (DCX, green) from a segment of dorsolateral STR. Maximum projection of 66 optical planes that are part of the reconstruction of 10 serial coronal sections (50 µm).

(G) IHC localization (peroxidase-DAB staining) of DCX$^+$ cells clustered along WM tracts of STR (epoxy semi-thin coronal section).

(H) Representative TEM microphotograph of a migrating NB along striatal myelin bundles, characterized by a nucleus with dispersed chromatin, smooth scant cytoplasm and the presence of authophagosomes (yellow arrow).

Dots in (D and E) represent different mice. Animals: $n = 3$ (male and female). Data represent mean ± SEM. *$p \leq 0.05$, **$p \leq 0.01$, and ***$p \leq 0.001$ (one-way ANOVA). Scale bars: (A–C) 500 and 50 µm, (F) 100 µm, and (H) 5 µm.

DCX with Ki67, BrdU, or MASH1, indicating that DCX$^+$ migrating NBs are distinct from MASH1$^+$ progenitors and do not proliferate. A small percentage of DCX$^+$ cells co-expresses OLIG2 (Figure 4B, arrow), a finding also reported in previous studies (del Águila et al., 2022; Jablonska et al., 2010). Interestingly, clustering of DCX$^+$ NBs according to their morphology indicated that those accumulated inside myelin bundles preserve an immature elongated phenotype, organized either in chains or as unipolar or bipolar single cells (Figure 4A). Occasionally, DCX$^+$ cells localized outside myelin bundles in the surrounding gray matter parenchyma exhibit a more differentiated neuronal phenotype, extending long processes and multiple dendrites (Figure 4A″; Figure 2B, red arrow) and a subpopulation co-express the mature neuronal markers i.e., NeuN (Figures 4C and 4D), and the marker of MSNs CTIP2 (Figure 4E). In some cases, NBs outside myelin structures have been observed to extend cytoplasmic projections

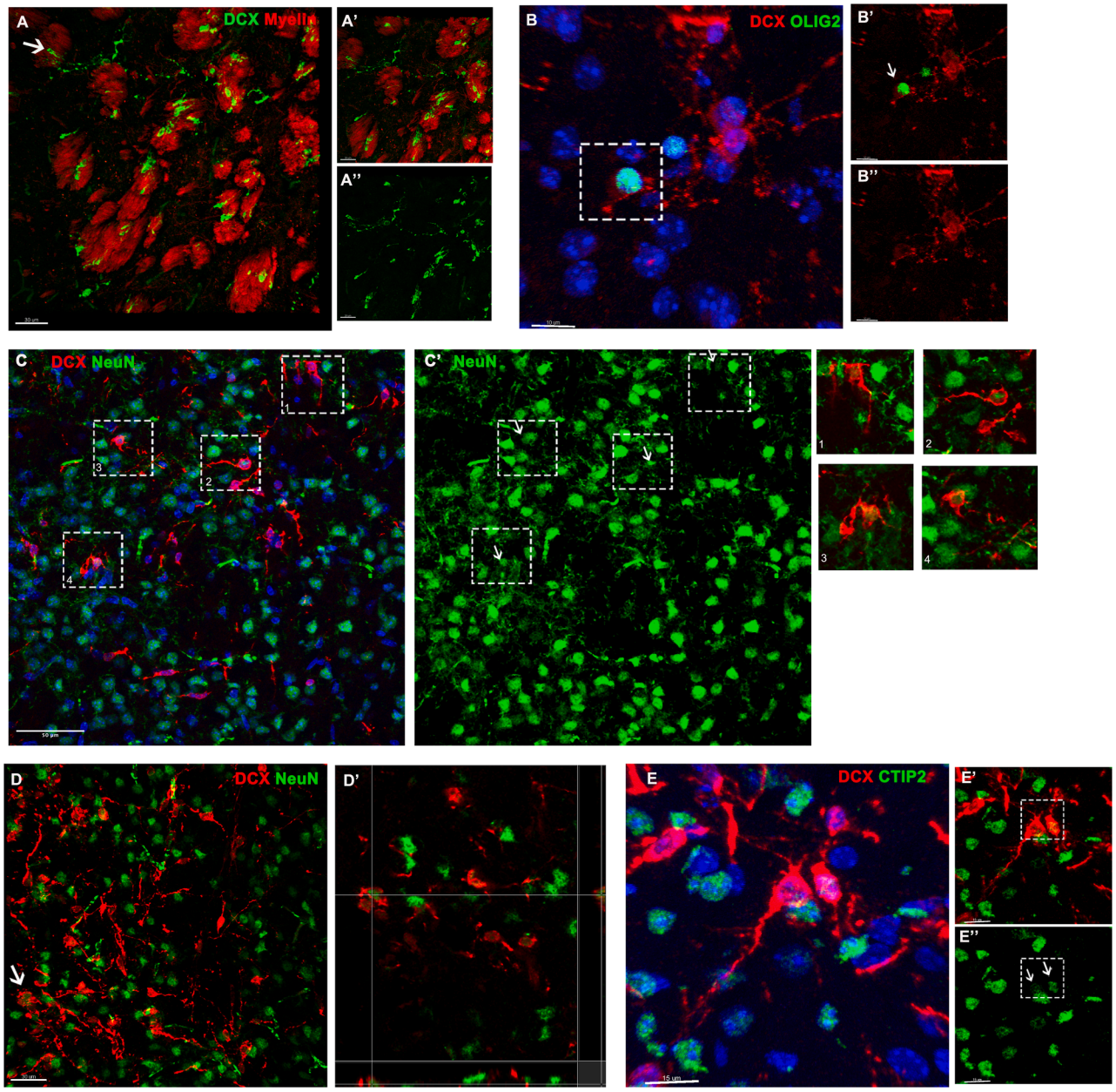

Figure 4. differentiation of NBs in striatal grey matter

(A) NBs (DCX) in and out of striatal myelin tracks (Dil lipophilic labeling). White arrow indicates a cytoplasmic projection toward a myelin tract.

(B) Few DCX+ cells (arrow) express OLIG2.

(C and D) Several DCX+ cells in gray matter, co-expressing NeuN. (D′) Orthogonal view of a cell (arrow in D) expressing DCX and NeuN.

(E–E′) NBs (DCX) expressing CTIP2 (arrows). DAPI (blue).

Scale bars: (A and D) 30 μm, (A′–A″) 20 μm, (B–B″) 10 μm, (C) 50 μm, and (E–E″) 15 μm.

(Figure 4A, white arrow). All the aforementioned observations are highlighting a strong polarization of migratory NBs toward myelin substrates and further suggest that cell fate decisions and the maturation status of neuronal progenitors are influenced by their spatial distribution in diverse cellular substrates.

AraC induces acute neuroiflammation with peripheral cell infiltration and tissue loss of the periventricular regions

A pronounced enlargement of brain ventricles was observed at 6 weeks p.i (Figure 5A). To quantify this finding, we performed measurements of the ventricular,

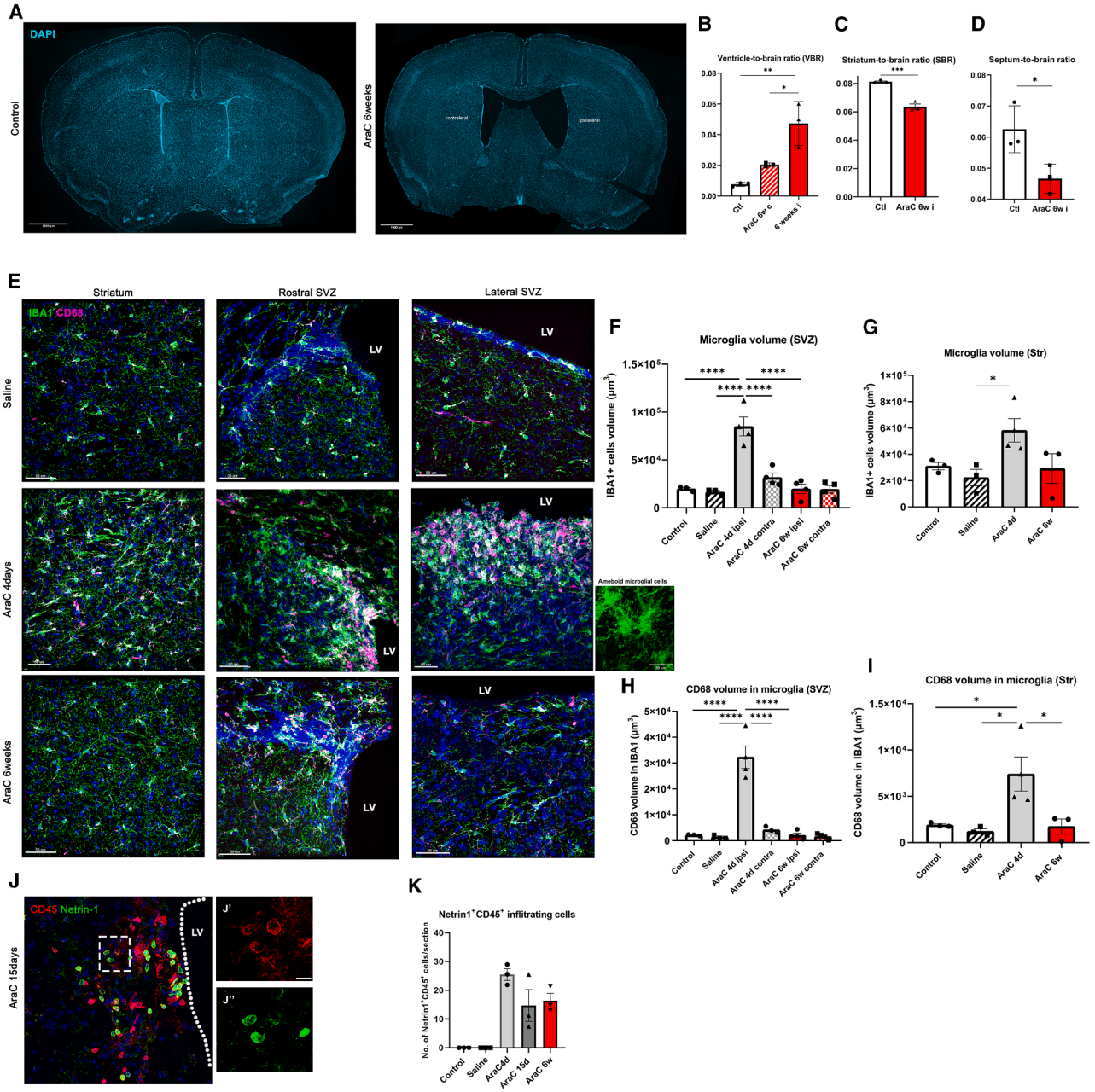

Figure 5. Neuroinflammation with peripheral cell infiltration and periventricular tissue loss

(A) IHC representative images of whole brain coronal sections of Ctl and AraC 6-week groups illustrating the enlargement of ventricles, and shrinkage of adjacent striatal and septal areas.

(B–D) Quantification of the ratio of (B–D). (B) Ventricles-to-brain areas (one-way ANOVA), (C) STR-to-brain areas, and (D) septum-to-brain areas (Student's t test).

(E–I) (E) IHC representative images of IBA1 and CD68 in STR, rostral, and lateral SVZ. Inset is a magnification of IBA1 in AraC, 4 days, showing microglia with ameboid morphology. Quantification of IBA1 microglia volume in the (F) SVZ and (G) STR (one-way ANOVA). Quantification of CD68 phagocytic microglia volume in the SVZ (H) and STR (I) (one-way ANOVA).

(J) IHC illustrating cells double-stained for CD45 and netrin-1 lying in SVZ and adjacent regions 15 days p.i.

(K) Quantification of the number of $CD45^+$/$netrin^+$ cells per section.

Dots in (B–D, F–I, and K) represent different mice. Animals: $n = 3–4$ (male and female). Data represents mean ± SEM. $*p \leq 0.05$, $**p \leq 0.01$, $***p \leq 0.001$, and $****p \leq 0.0001$ (one-way ANOVA and Student's t test for C and D). Scale bars: (A) 1,000 µm, (E) 50 µm, (inset) 20 µm, (J) 30 µm, and (J') 10 µm.

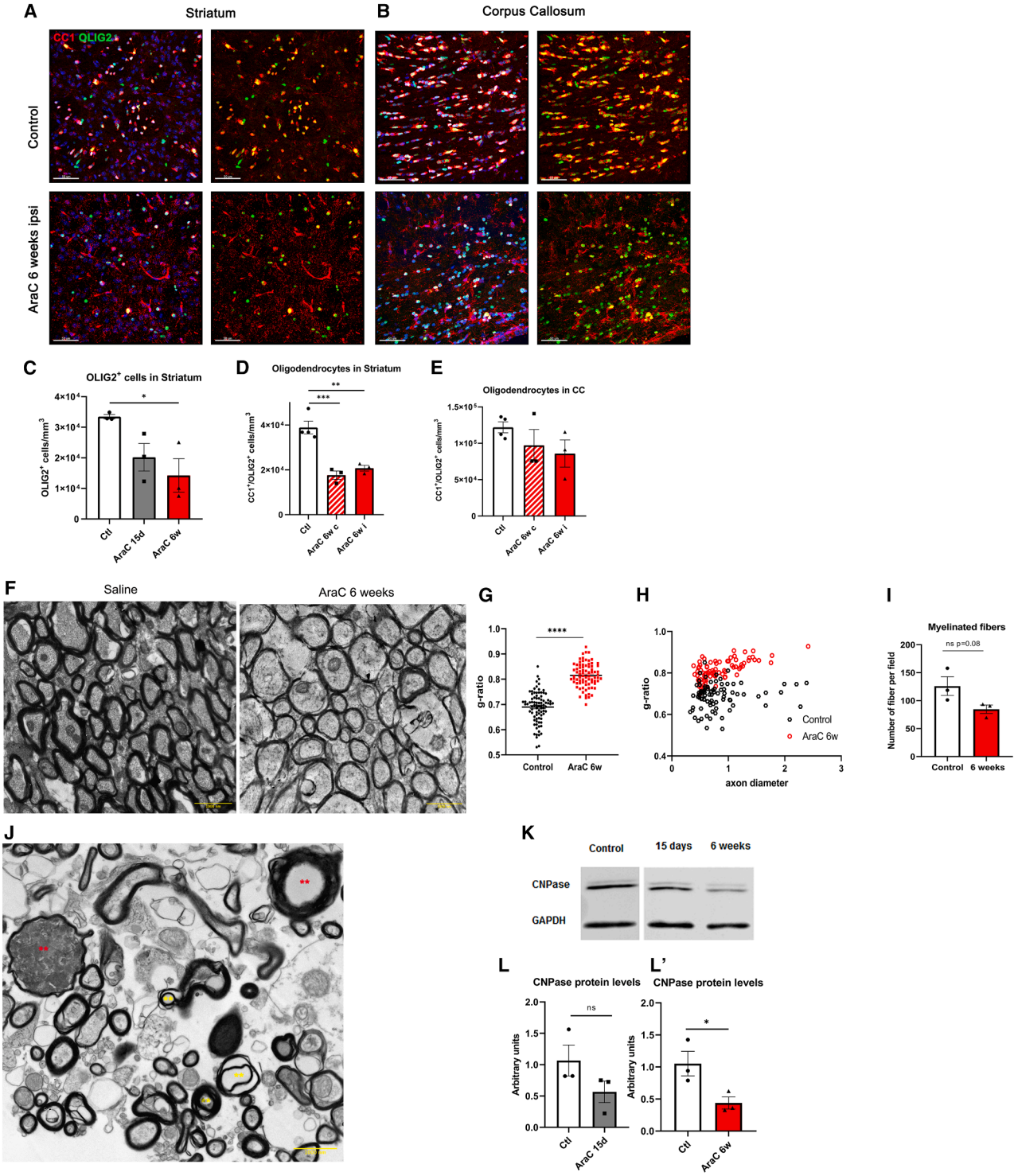

Figure 6. Impaired oligodentrocyte lineage progression and myelin structure dysregulation

(A and B) Representative confocal images of OLIG2$^+$/CC1$^+$ cells in (A) STR and (B) CC.

(C–E) (C) Quantification of the density of OLIG2$^+$ cells in the STR. Quantification of the density of CC1$^+$/OLIG2$^+$ cells in (D) STR and (E) CC.

(F) Representative TEM microphotographs of the myelinated axons.

(G) Quantification of myelin sheath thickness by g-ratio (Mann-Whitney test).

(legend continued on next page)

striatal and septal areas. In 6 weeks, ventricle-to-brain area ratio is significantly increased ipsilaterally, while the contralateral side exhibits no significant difference (Figure 5B). Since the average area of whole brain sections remained unchanged, we hypothesized that the observed ventriculomegaly should be attributed to tissue loss. To elucidate this, we measured the ipsilateral striatal and septal areas, both significantly decreased, indicating ongoing degeneration (Figures 5C and 5D).

As known from previous reports, neuroinflammation stands as the starting point of a series of events that can ultimately lead to tissue loss, thus considered a significant risk factor for neurodegeneration (Zhang et al., 2023). We therefore evaluated SVZ neuroinflammation in our model, and our data reveal a robust acute neuroinflammatory response along the SVZ dorsoventral axis at 4 days. This response is characterized by pronounced microglial activation (Figure 5E), particularly near the ventricular and septal walls, and into surrounding parenchyma. Quantification of microglial activation revealed a significant transient increase in the volume of IBA1$^+$ cells at 4 days, which is evident both at the SVZ and the more distal striatal area (Figures 5F and 5G). This enhanced activation was accompanied by increased phagocytic phenotype, as evidenced by increase expression of the CD68 in SVZ and STR (Figures 5E–5I) and a shift to ameboid morphology, indicating high activation at 4 days p.i. (Figure 5E, inset). However, by 6 weeks, microglial cells have returned to their resting state with distinct ramified morphology (Figures 5E–5I).

Emerging data indicate that several chemotherapeutic agents are detectable within the CNS (Jacus et al., 2016; Wardill et al., 2016), suggesting a potential disruption of the CNS barriers, which results in infiltration of peripheral cells into the brain. To test whether this is also the case in our model, we immunostained for CD45 (leukocytes) and CD3 (T cells) to assess peripheral cell infiltration inside the brain. Thus, we examined their presence in the choroid plexus (CP), which we considered more susceptible to disruption due to its location inside the ventricles and periventricular parenchyma. Indeed, a presence of CD3$^+$ cells (Figure S2B) and CD45$^+$ (Figure S2C), as early as 4 days p.i., is prominently noted within and crossing the CP, indicating a compromise in the integrity of the blood-cerebrospinal fluid barrier (B-CSF). As anticipated, the control (Ctl) group showed very few, if any, peripheral cells at the CP entry point (Figure S2A) or the neighboring striatal parenchyma (Figure S2A′). Interestingly, a population of CD45$^+$/CD3$^-$ immune cells infiltrated through CP (Figure S2C′) to the brain parenchyma, expressing netrin-1, known to play a role in axon guidance, as soon as 4 days after AraC infusion (Figures 5J–5K and S2D–S2E′), with its expression persisting for up to 6 weeks (Figures 5K, S2F, and S2F′). Particularly, this population is localized in the lateral walls, CC and striatal parenchyma, often arranged in characteristic stacks in or around vessels (Figures S2F and S2F′), indicating that, in addition to the loosening of the B-CSF, BBB leakage may occur.

Dysregulation of oligodendrocyte lineage dynamics and myelin homeostasis

Given the significant accumulation of ectopic NBs primarily along striatal myelin tracts, we assessed their impact on myelin and the properties of myelinating cells. Chemotherapeutics are known to cause oligodendrocyte lineage dysregulation due to neuroinflammation, leading to disrupted myelination (Gibson et al., 2019). To determine if this occurs in our model, we quantified OLIG2$^+$ cells in the STR post-AraC infusion. Our results indicate a reduction in the number of OLIG2$^+$ cells starting from the 15-day time point, which appears to be significant at 6 weeks (Figures 6A and 6C). We then estimated the number of mature oligodendrocytes in the STR and CC by co-immunostaining with CC1 and OLIG2. At 6 weeks, mature CC1$^+$/OLIG2$^+$ oligodendrocytes we significantly reduced in both ipsilateral and contralateral STR (Figures 6A and 6D), a similar trend was observed in the CC, but was not significant (Figures 6B and 6E). To decipher whether the loss of mature oligodendrocytes affects myelination, we used transmission electron microscopy (TEM) to scrutinize brain ultrastructure. Myelin sheath thickness was markedly reduced in the CC (Figure 6F), as reflected by increased G-ratio (Figures 6G and 6H), 6 weeks following AraC administration. Reduced diameter of myelin sheath is accompanied by the presence of infolded myelin loops (Figure 6J, yellow stars) and degenerated axons (Figure 6J, red stars) indicative of dysmyelination and neurodegeneration respectively. Myelinated axon numbers in the CC

(H) Scatterplot of individual g-ratio versus axonal diameter. The g-ratio of each measured fiber is indicated by a single circle.
(I) Quantification of myelinated axons per field.
(J) Representative image of degenerated axons (red stars) and infolded myelin loops (yellow stars) observed in an AraC 6-week group.
(K) Representative image of western blot bands for CNPase and GAPDH (same blot).
(L–L′) Quantification of CNPase protein levels normalized to GAPDH and expressed relative to Ctl group.
Dots in (C–E, I, and L–L′) represent different mice and in (G and H) represent different axons. Animals: n = 3–4 (male and female). Data represents mean ± SEM. ns, not significant; *$p \leq 0.05$, **$p \leq 0.01$, ***$p \leq 0.001$, and ****$p \leq 0.00010001$ (one-way ANOVA and Student's t test for L–L′). Scale bars: (A and B) 50 μm and (F and J) 1 μm.

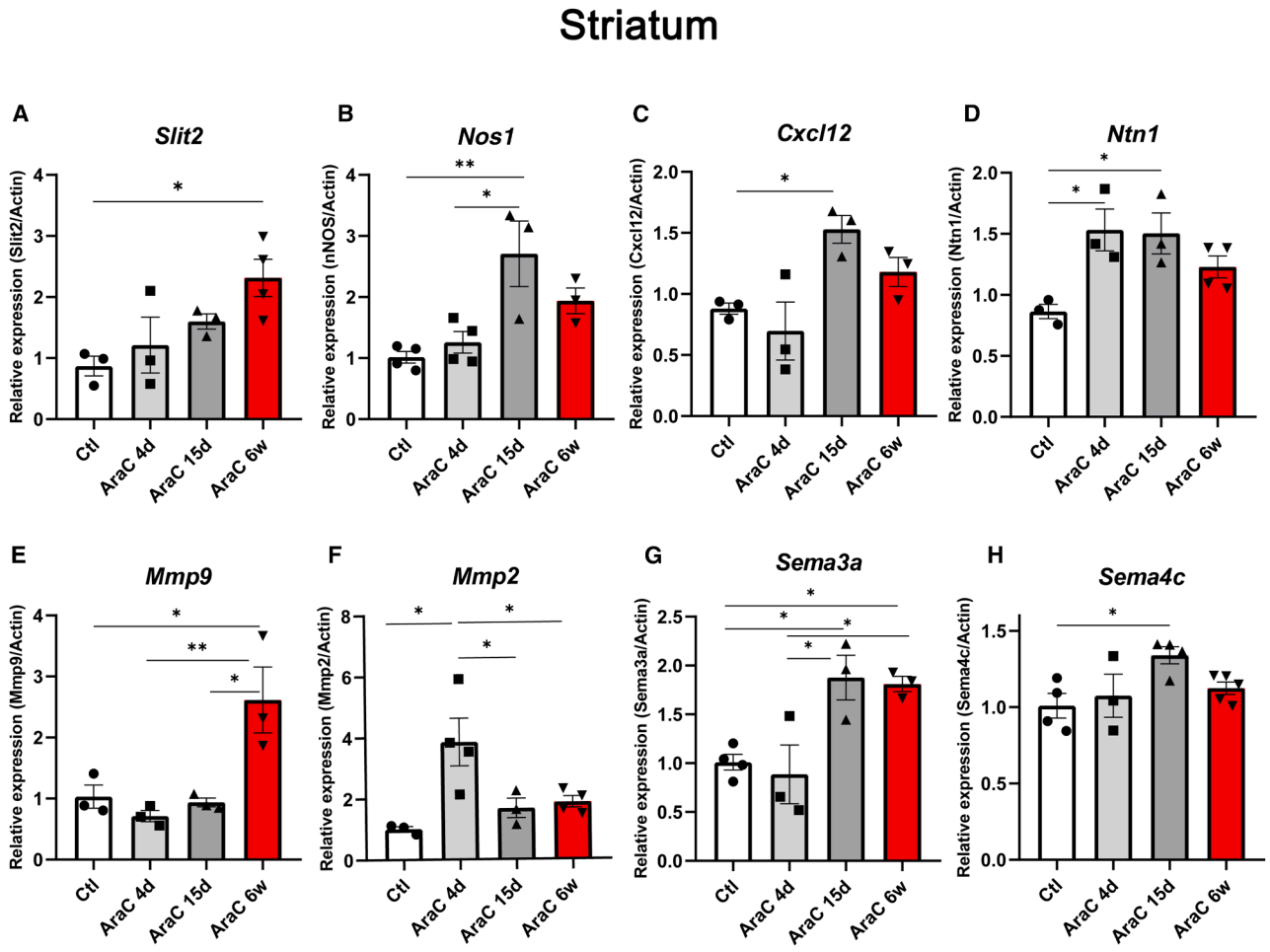

Figure 7. Expression profiling of migration-regulating genes by quantitative real-time RT-PCR

Quantification of mRNA levels of target genes in the STR, including *Slit2*, *Nos1*, *Cxcl12*, *Ntn1*, *Mmp9*, *Mmp2*, *Sema3a*, and *Sema4c*, shown in (A–H).

Dots in (A–H) represent different mice. Animals: $n = 3–5$ (male and female) Data represent mean ± SEM. $^{*}p \leq 0.05$ and $^{**}p \leq 0.01$ (one-way ANOVA).

declined slightly, but not significantly (Figure 6I). In accordance with the EM findings, the protein levels of CNPase myelin-associated enzyme were found to decrease, with a significant reduction at 6 weeks p.i (Figures 6K, 6L, and 6L′).

Differential expression of genes associated with the regulation of migration

Considering the aberrant migration from the SVZ neurogenic niche after AraC administration, we aimed to explore the underlying molecular mechanisms. Thus, we assessed mRNA levels of genes related to migration, neurogenic commitment, and positioning of newborn neurons in the ipsilateral striatum at three time points post-treatment. Initially, we evaluated the expression of *Slit2* that is involved in the regulation of migration and axonal projection in homeostasis and injury (Kaneko et al., 2018). Its elevated trend through the timeline with a significant increase in 6 weeks, aligns with our data for the presence of DCX+ ectopic cells in the striatum, making Slit2 a potential important factor that drives this aberrant migration (Figure 7A). Subsequently, we explored the expression of *Nos1*, known for its role in suppressing proliferation of NSCs and in promoting neuronal fate commitment and differentiation (Jin et al., 2017). Our analysis revealed an increase of its expression levels 15 days p.i. (Figure 7B), suggesting a response to chemical injury favoring neurogenic commitment of NSCs. Driven by the migration alterations neuroblasts exhibit upon AraC treatment, we next assessed the expression levels of *Cxcl12* (also known as SDF1), ligand of CXCR4 receptor, a well-established chemokine that promotes migration (Mimura-Yamamoto et al.,

2017). *Cxcl12* levels in the striatum show a notable increase at 15 days (Figure 7C) concomitant with the observed ectopic neuroblasts' migration. Since NB migration depends on extracellular matrix (ECM) remodeling via metalloprotease activation, which mediates the chemotactic function of SDF-1 (Janowska-Wieczorek et al., 2000), we next examined MMP2 and MMP9. Interestingly, *Mmp2* expression is increased in striatum only 4 days p.i. (Figure 7F), while *Mmp9* levels are elevated only after 6 weeks in the striatum (Figure 7E). These differences are in line with previous reports of a transient increase of *Mmp2* levels during early BBB breakdown (Chang et al., 2003), whereas *Mmp9* seems to play a role in delayed damage (Yang et al., 2007). Apart from durotactic cues, such as MMPs, we examined the chemotactic molecule semaphorin 3A mostly known for its role in dendritic branching (Ng et al., 2013). The mRNA expression of *Sema3a* in the striatum indicates a persistent notable increase from 15 days up to 6 weeks as compared to the control and 4-day groups (Figure 7G). Likewise, the expression of *Ntn1*, an axon guidance cue, shows a significant increase as early as 4 days that persists up to 6 weeks, though at a lower level (Figure 6D). Increased *Ntn1* expression might be attributed to the aforementioned observation of a netrin-1+ population of infiltrating cells (Figures 7I–7G) and suggest their potential role in ectopic neuroblasts migration, as part of their contribution in neuronal repair as proposed in other studies (Madison et al., 2000). Lastly, driven by a recent study that proposed that plexin B2-semaphorin 4C complex plays a role in glioblastoma cell invasion into fiber tracts (Huang et al., 2021), we examined the expression of *Sema4c* in our model. Our results indicate a significant increase of *Sema4c* levels 15 days p.i (Figure 7H).

Taken together, our data indicate that the factors exhibiting altered transcriptional levels are related to the guidance of migratory neuroblasts and mostly start being affected in the mid-term of 15 days p.i, while they remain elevated at 6 weeks. On the other hand, molecules linked to BBB rapture and peripheral cells' infiltration after injury, such as MMPs and netrin-1, present a more diverse time-related pattern, which likely reflects the long-term disturbance of homeostasis in our model.

DISCUSSION

Our experimental model, involving intraventricular infusions of the antimitotic agent AraC—a compound commonly used in chemotherapeutic protocols (Reese and Schiller, 2013)—offers valuable insights into the brain's adaptive responses to chemical injury and mimics features commonly observed in chemo brain. Notably, this approach reveals previously uncharacterized adult neurogenesis-related alternative migratory routes mobilized following brain injury. Importantly, we report for the first time a specific preference for a large number of ectopically recruited neuroblasts along the rostro-caudal axis of striatal IC fibers, as well as the latent activation of a ventral migratory stream through the NAc toward the anterior commissure, possibly attracted to and involved in the support or repair of compromised myelin structures. While previous studies have shown that brain insults, such as stroke, mobilize SVZ neurogenesis toward injured sites, often migrating along vasculature (Ohab et al., 2006), and that demyelinating conditions recruit SVZ-derived cells mainly differentiating into oligodendrocytes (El Waly et al., 2022), our findings highlight the activation of alternative long-distance migration pathways. These pathways enable a substantial number of newborn neurons to migrate over extended time frames using myelin tracts, which may play a supportive role in maintaining or repairing the structural integrity compromised by injury.

Chemotherapeutic agents induce cytotoxicity through DNA damage, reactive oxygen species, and stress responses, with ependymal cells being especially vulnerable (Ren et al., 2019; Was et al., 2022). Our model reproduces acute and persistent ependymal loss and ventricular wall degeneration, leading to ventricular dilation characteristic of hydrocephalus *ex vacuo*—a pathology common in stroke and neurodegenerative conditions (Reider-Groswasser et al., 2002). These alterations, linked to cognitive impairment, are also documented in aging and injured human brains (Shook et al., 2014; Todd et al., 2018). The balance between NSC pool maintenance and cellular differentiation depends on microenvironmental signals received not only from intercellular interactions within the neurogenic niche, but also from the CSF and vasculature (Chaker et al., 2016). In this light, disruption of the ependymal cells ipsilaterally is, among other factors, responsible for the change in the rate of NSC proliferation and differentiation. In accordance with this line, in our model, we observe reduced proliferation levels of the total NSC population up to 6 weeks after AraC administration on both sides; however, to a lesser extent contralaterally. This finding suggests that with the scheme we applied, along with the significant reduction in the number of rapidly proliferating NSCs, the pool of slowly proliferating NSCs is also affected, since previous data have shown that following elimination only of the rapidly proliferating SVZ cells with antimitotic agents, the neurogenic niche is regenerated in less than 10 days due to recruitment of slowly proliferating NSCs (Doetsch et al., 1999). Notably, proliferation keeps decreasing throughout the weeks also on the contralateral side, possibly reflecting a long-term imbalance of the extrinsic cues that regulate SVZ niche dynamics such as

those derived from CSF, blood vessels, neuronal projections, and cell-cell interactions.

Of note, the alterations in the cellular scaffold on which the NBs migrate along with the imbalance of factors they receive from the niche microenvironment, affect their migratory behavior. Previous studies have reported that in response to injury, NBs are recruited to non-neurogenic lesioned parenchymal regions in an attempt to support regeneration (Arvidsson et al., 2002; Parent et al., 2002). As previously reported the neurogenesis toward lesioned sites significantly impacts the RMS-OB pathway by diverting NBs from their typical destination (Lindvall and Kokaia, 2015; Young et al., 2011). This redirection alters migration dynamics ultimately leading to decreased OB neurogenesis, a phenomenon also observed in our model. Neuroblasts' redirection could be also attributed to netrin-1, a guidance molecule shown to promote the migration of SVZ-derived neuroblasts toward demyelinating lesions (Cayre et al., 2013). The role of netrin-1$^+$ peripheral cells is not yet elucidated, but its expression may suggest potential involvement in neural regeneration, as proposed by studies in other tissues (Ding et al., 2021; Gao et al., 2021). Interestingly, other studies have reported a possible connection between CD45$^+$ cells' presence in the SVZ and NB emigration from the niche (Goings et al., 2008).

A key finding in our study is the ectopic appearance of NBs and their presence along myelin fibers in CC, STR, and AC. Myelin fibers are known to serve as a permissive migration substrate for NBs, with WM also reported as a potential site for secondary neurogenesis (Cayre et al., 2006, 2010; Costine et al., 2015; Luzzati et al., 2014). The myelinated environment biases cells toward migratory states (Chen et al., 2015) while inhibiting neuronal maturation (Hosseini et al., 2022). Conversely, the emergence of a subpopulation of more differentiated NBs in the striatal gray matter is possibly attributed to the permissive ECM substrates (Mruthyunjaya et al., 2010; O'Connor et al., 2025) and neurotrophic factors secreted from neighboring neurons.

Many studies have reported that significant neuronal loss due to damage in areas adjacent to neurogenic niches could redirect the fate of stem cell-derived NBs not only to migrate to the damaged area but also to differentiate into regionally appropriate neuronal subtypes such as midbrain dopamine neurons (Zhao et al., 2003) and MSNs (Arvidsson et al., 2002; Parent et al., 2002). However, this hypothesis is still controversial, with other studies supporting that ectopic NBs in STR cannot alter their differentiation potential to become striatal projection neurons, but rather maintain their identity as OB interneurons (Liu et al., 2009). Our results indicate that a fraction of newborn neurons acquires more mature characteristics and may adopt a striatal projection neuron identity, localizing exclusively within the gray matter parenchyma. Previous studies in CNS injury models also reported neuronal maturation, evidenced by NeuN and GAD67 expression, occurring exclusively in gray matter (Cummings et al., 2005).

The presence of radial glia-like cells, and NBs in the ventral part of the SVZ (Sundholm-Peters et al., 2004) together with the mapping of different transcription factors expressed along the SVZ dorsoventral axis (Chaker et al., 2016; Merkle et al., 2007), highlight the cell heterogeneity between the dorsal and ventral parts of the SVZ. These distinct SVZ domains may exhibit a greater extent of functional diversity than originally thought, a hypothesis reinforced by arising secondary migratory routes from ventral SVZ, either producing newborn, postnatal and adult MSNs in NAc (García-González et al., 2021) or granule neurons in the Calleja islands and olfactory tubercle postnatally (De Marchis et al., 2004). In this light, the extensive migration of NBs from the ventral SVZ to the NAc as uncovered by the intraventricular administration of AraC, reflects an inactive, under physiological conditions, migratory pathway toward subcortical brain regions.

Recent studies highlight the existence of latent neurogenic potential in striatal and cortical astrocytes following injury or genetic manipulation (Fogli et al., 2024; Magnusson et al., 2014; Nato et al., 2015; Zamboni et al., 2020; Zhang et al., 2022). However, the absence of proliferating clusters in the STR within our experimental model, contrary to findings in other studies that report local progenitor proliferation, suggests that local cell *trans*-differentiation is unlikely. Nevertheless, reviewing published images from studies of local neurogenesis (Magnusson et al., 2014; Zhang et al., 2022; Fogli et al., 2024), we noted that NBs derived from striatal astrocytes exhibited a strong tropism fort the myelin bundles of the STR. However, this finding was not pointed out and discussed in any of these studies. Under this light, the possibility that a population of local astrocytes lining along myelin tracts has a distinct neurogenic potential cannot be ruled out.

Changes in myelin integrity have been pointed out as a significant feature of chemo brain pathology (Wang et al., 2013), particularly associated with long-term neurological deficits (Anderson et al., 2000; Winocur et al., 2006). Recent findings from Gibson and colleagues, suggest that systemic administration of methotrexate, another chemotherapeutic agent, results in myelin sheath defects along with a persistent glia dysregulation mediated by microglia activation (Gibson et al., 2019). Our results are in accordance with these observations, showing a similar dysregulation of oligodendrocyte lineage and deficits in

myelin ultrastructure, raising the question of whether NBs accumulation is directed toward WM tracts in an attempt to support reparative mechanisms possibly taking place. It has been proposed that upon demyelination, SVZ NBs can be rerouted toward lesioned sites undergoing a spontaneous *trans*-differentiation to oligodendrocytes (Jablonska et al., 2010; El Waly et al., 2022). The few ectopic DCX +/OLIG2^{+} cells along with the increased *Nos1* expression levels—known to promote neuronal fate commitment and differentiation—found in our model do not point to this direction; however, fate-mapping approaches would be more appropriate to evaluate this possibility. Interestingly, recent findings provide evidence on the role of ectopic NBs during ischemia in providing trophic support for neural repair through VEGF production (Williamson et al., 2023), rather than a direct neuronal replacement that was the predominant hypothesis. This is particularly interesting considering that in most studies, even though NBs can acquire mature characteristics, their nature is transient, and only few are integrated into the neural circuits (Yamashita et al., 2006). In this view, the retention of the large number of NBs along the WM tracts in our model may suggest a protective role on the affected axons. Yet, further experiments are needed to elucidate such hypotheses.

Limitations of the study

Viral tracing was performed using the AAV-GFAP-Cre vector (pAAV.GFAP.Cre.WPRE.hGH) injected into the STR or LVs of ROSA26-YFP mice to label NCSs and/or neurogenic astrocytes. However, we abandoned this approach due to extensive off-target neuronal labeling, aligning with recent findings that question the specificity of AAV-based astrocyte lineage-tracing approaches (Wang et al., 2021).

Conclusions: Future directions

Elucidating the mechanisms that direct NB migration shifts is crucial for developing effective therapies for brain injury. Myelin tracts appear to provide a suitable substrate for NB migration, and a subpopulation of these NBs can differentiate into region-specific mature neurons. Thus, creating myelin-based scaffolds to steer NB migration over long distances to specific injury sites could be highly valuable. Additionally, WM tracts serve as invasion routes for glioblastoma cells, causing detrimental effects (Cuddapah et al., 2014). Given that the human SVZ may be a niche for tumor-initiating glioma cells (Piccirillo et al., 2015), shared mechanisms underlying aberrant migration after brain injury and glioblastoma invasion might be uncovered. By highlighting multiple guidance and tissue remodeling cues involved in injury response, we gain initial insight into the complex processes that govern NB positioning and fate determination.

METHODS

Animal procedures

All surgeries and experimental procedures were performed in compliance with European and National legislation for Laboratory Animal Use (Guideline 2010/63/EE and Greek Law 56/2013) according to FELASA recommendations for euthanasia and the Guide for Care and Use of Laboratory Animals of the National Institutes of Health. All protocols were approved by the Institutional Animal Care and Use Committee of the Hellenic Pasteur Institute (Animal House Establishment Code: EL 25 BIO 013) and the License No 5677/25-09-2012 for experimentation was issued by the Greek authorities (Veterinary Department of Athens Prefecture).

Stereotaxic injection

Animals were anesthetized with 4% isoflurane, positioned in the stereotaxic apparatus and injected with 10 μl Hamilton syringe. Injection coordinates are as follows: AraC 3% (w/v) (6μL; dissolved in 0.9% NaCl) AP: −0.3 mm, ML: +1.0, DV: −2.5.

3D reconstructions

3D reconstructions were performed as described before (Luzzati et al., 2011).

Extended experimental procedures are described in supplemental information.

RESOURCE AVAILABILITY

Lead contact

Further information and requests for resources and reagents should be directed to the lead contact, Dimitra Thomaidou (thomaidou@pasteur.gr).

Materials availability

This study did not generate any unique reagents.

Data and code availability

Primary data and information to re-analyze them are available from the lead contact upon request.

ACKNOWLEDGMENTS

We thank Dr. Evangelia Xingi (Bioimaging Unit, HPI) for technical support in imaging and image analysis and Dr. Anna Haroniti for her support in western blot experiments. This work was supported by "BIOIMAGING-GR (MIS 5002755)," co-financed by Greece and the EU Regional Development Fund, the General Secretariat for Research and Innovation under the National research network for neurodegenerative diseases, National Recovery and Resilience Plan Greece 2.0 (TAA) and European Union, Next Generation EU, TAEDR-0535850—BrainPrecision awarded to D.T., and by the Nostos Foundation PhD Fellowship and Network of European Neuroscience Schools (NENS) Fellowship awarded to I.T.

AUTHOR CONTRIBUTIONS

Conceptualization, I.T. and D.T.; *in vivo* experiments, I.T.; 3D reconstruction, F.L. and I.T.; transmission electron analysis, P.N. K., S.H., and V.G.G.; data analysis, I.T. and M.M.; writing – original draft, I.T. and D.T.; writing – review and editing, I.T., D.T., F.L., P.N. K., and S.H.; supervision and funding acquisition, D.T.

DECLARATION OF INTERESTS

The authors declare no competing interests.

SUPPLEMENTAL INFORMATION

Supplemental information can be found online at https://doi.org/10.1016/j.stemcr.2025.102636.

Received: January 15, 2025
Revised: August 11, 2025
Accepted: August 11, 2025
Published: September 9, 2025

REFERENCES

del Águila, Á., Adam, M., Ullom, K., Shaw, N., Qin, S., Ehrman, J., Nardini, D., Salomone, J., Gebelein, B., Lu, Q.R., et al. (2022). OLIG2 defines a subset of neural stem cells that produce specific olfactory bulb interneuron subtypes in the subventricular zone of adult mice. Development *149*, dev200028. https://doi.org/10.1242/dev.200028.

Anderson, V.A., Godber, T., Smibert, E., Weiskop, S., and Ekert, H. (2000). Cognitive and academic outcome following cranial irradiation and chemotherapy in children: a longitudinal study. Br. J. Cancer *82*, 255–262. https://doi.org/10.1054/bjoc.1999.0912.

Arvidsson, A., Collin, T., Kirik, D., Kokaia, Z., and Lindvall, O. (2002). Neuronal replacement from endogenous precursors in the adult brain after stroke. Nat. Med. *8*, 963–970. https://doi.org/10.1038/nm747.

Bressan, C., Pecora, A., Gagnon, D., Snapyan, M., Labrecque, S., De Koninck, P., Parent, M., and Saghatelyan, A. (2020). The dynamic interplay between ATP/ADP levels and autophagy sustain neuronal migration in vivo. eLife *9*, e56006. https://doi.org/10.7554/eLife.56006.

Cayre, M., Bancila, M., Virard, I., Borges, A., and Durbec, P. (2006). Migrating and myelinating potential of subventricular zone neural progenitor cells in white matter tracts of the adult rodent brain. Mol. Cell. Neurosci. *31*, 748–758. https://doi.org/10.1016/j.mcn.2006.01.004.

Cayre, M., Canoll, P., and Goldman, J.E. (2010). Cell Migration in the Normal and Pathological Postnatal Mammalian Brain. Prog Neurobiol. *88*, 41–63. https://doi.org/10.1016/j.pneurobio.2009.02.001.Cell.

Cayre, M., Courtès, S., Martineau, F., Giordano, M., Arnaud, K., Zamaron, A., and Durbec, P. (2013). Netrin 1 contributes to vascular remodeling in the subventricular zone and promotes progenitor emigration after demyelination. Development (Camb.) *140*, 3107–3117. https://doi.org/10.1242/DEV.092999.

Chaker, Z., Codega, P., and Doetsch, F. (2016). A mosaic world: puzzles revealed by adult neural stem cell heterogeneity. WIREs Dev. Biol. *5*, 640–658. https://doi.org/10.1002/wdev.248.

Chang, D.-I., Hosomi, N., Lucero, J., Heo, J.-H., Abumiya, T., Mazar, A.P., and del Zoppo, G.J. (2003). Activation Systems for Latent Matrix Metalloproteinase-2 are Upregulated Immediately after Focal Cerebral Ischemia. J. Cereb. Blood Flow Metab. *23*, 1408–1419. https://doi.org/10.1097/01.WCB.0000091765.61714.30.

Chen, C.-C.V., Hsu, Y.-H., Jayaseema, D.M., Chen, J.-Y.J., Hueng, D.-Y., and Chang, C. (2015). White matter tracts for the trafficking of neural progenitor cells characterized by cellular MRI and immunohistology: the role of CXCL12/CXCR4 signaling. Brain Struct. Funct. *220*, 2073–2085. https://doi.org/10.1007/s00429-014-0770-4.

Costine, B.A., Missios, S., Taylor, S.R., McGuone, D., Smith, C.M., Dodge, C.P., Harris, B.T., and Duhaime, A.C. (2015). The subventricular zone in the immature piglet brain: Anatomy and exodus of neuroblasts into white matter after traumatic brain injury. Dev. Neurosci. *37*, 115–130. https://doi.org/10.1159/000369091.

Cuddapah, V.A., Robel, S., Watkins, S., and Sontheimer, H. (2014). A neurocentric perspective on glioma invasion. Nat. Rev. Neurosci. *15*, 455–465. https://doi.org/10.1038/nrn3765.

Cummings, B.J., Uchida, N., Tamaki, S.J., Salazar, D.L., Hooshmand, M., Summers, R., Gage, F.H., and Anderson, A.J. (2005). Human neural stem cells differentiate and promote locomotor recovery in spinal cord-injured mice. Proc. Natl. Acad. Sci. USA *102*, 14069–14074. https://doi.org/10.1073/pnas.0507063102.

Ding, S., Guo, X., Zhu, L., Wang, J., Li, T., Yu, Q., and Zhang, X. (2021). Macrophage-derived netrin-1 contributes to endometriosis- associated pain. Ann. Transl. Med. *9*, 29. https://doi.org/10.21037/atm-20-2161.

Doetsch, F., Garcia-Verdugo, J.M., and Alvarez-Buylla, A. (1999). Regeneration of a germinal layer in the adult mammalian brain. Proc. Natl. Acad. Sci. USA *96*, 11619–11624. https://doi.org/10.1073/pnas.96.20.11619.

Fogli, M., Nato, G., Greulich, P., Pinto, J., Ribodino, M., Valsania, G., Peretto, P., Buffo, A., and Luzzati, F. (2024). Dynamic spatiotemporal activation of a pervasive neurogenic competence in striatal astrocytes supports continuous neurogenesis following injury. Stem Cell Rep. *19*, 1432–1450. https://doi.org/10.1016/j.stemcr.2024.08.006.

Gao, R., Peng, X., Perry, C., Sun, H., Ntokou, A., Ryu, C., Gomez, J.L., Reeves, B.C., Walia, A., Kaminski, N., et al. (2021). Macrophage-derived netrin-1 drives adrenergic nerve–associated lung fibrosis. J. Clin. Investig. *131*, e136542. https://doi.org/10.1172/JCI136542.

García-González, D., Dumitru, I., Zuccotti, A., Yen, T.Y., Herranz-Pérez, V., Tan, L.L., Neitz, A., García-Verdugo, J.M., Kuner, R., Alfonso, J., and Monyer, H. (2021). Neurogenesis of medium spiny neurons in the nucleus accumbens continues into adulthood and is enhanced by pathological pain. Mol. Psychiatry *26*, 4616–4632. https://doi.org/10.1038/s41380-020-0823-4.

Gibson, E.M., Nagaraja, S., Ocampo, A., Tam, L.T., Wood, L.S., Pallegar, P.N., Greene, J.J., Geraghty, A.C., Goldstein, A.K., Ni, L., et al. (2019). Methotrexate Chemotherapy Induces Persistent Tri-glial

Dysregulation that Underlies Chemotherapy-Related Cognitive Impairment. Cell *176*, 43–55.e13. https://doi.org/10.1016/j.cell.2018.10.049.

Goings, G.E., Greisman, A., James, R.E., Abram, L.K., Begolka, W.S., Miller, S.D., and Szele, F.G. (2008). Hematopoietic cell activation in the subventricular zone after Theiler's virus infection. J. Neuroinflammation *5*, 44. https://doi.org/10.1186/1742-2094-5-44.

Grade, S., and Götz, M. (2017). Neuronal replacement therapy: previous achievements and challenges ahead. NPJ Regen. Med. *2*, 29. https://doi.org/10.1038/s41536-017-0033-0.

Hosseini, S.M., Alizadeh, A., Shahsavani, N., Chopek, J., Ahlfors, J.-E., and Karimi-Abdolrezaee, S. (2022). Suppressing CSPG/LAR/PTPσ Axis Facilitates Neuronal Replacement and Synaptogenesis by Human Neural Precursor Grafts and Improves Recovery after Spinal Cord Injury. J. Neurosci. *42*, 3096–3121. https://doi.org/10.1523/JNEUROSCI.2177-21.2022.

Huang, Y., Tejero, R., Lee, V.K., Brusco, C., Hannah, T., Bertucci, T.B., Junqueira Alves, C., Katsyv, I., Kluge, M., Foty, R., et al. (2021). Plexin-B2 facilitates glioblastoma infiltration by modulating cell biomechanics. Commun. Biol. *4*, 145. https://doi.org/10.1038/s42003-021-01667-4.

Jablonska, B., Aguirre, A., Raymond, M., Szabo, G., Kitabatake, Y., Sailor, K.A., Ming, G.L., Song, H., and Gallo, V. (2010). Chordin-induced lineage plasticity of adult SVZ neuroblasts after demyelination. Nat. Neurosci. *13*, 541–550. https://doi.org/10.1038/NN.2536.

Jacus, M.O., Daryani, V.M., Harstead, K.E., Patel, Y.T., Throm, S.L., and Stewart, C.F. (2016). Pharmacokinetic Properties of Anticancer Agents for the Treatment of Central Nervous System Tumors: Update of the Literature. Clin. Pharmacokinet. *55*, 297–311. https://doi.org/10.1007/s40262-015-0319-6.

Janowska-Wieczorek, A., Marquez, L.A., Dobrowsky, A., Ratajczak, M.Z., and Cabuhat, M.L. (2000). Differential MMP and TIMP production by human marrow and peripheral blood CD34+ cells in response to chemokines. Exp. Hematol. *28*, 1274–1285. https://doi.org/10.1016/S0301-472X(00)00532-4.

Jin, K., Minami, M., Lan, J.Q., Mao, X.O., Batteur, S., Simon, R.P., and Greenberg, D.A. (2001). Neurogenesis in dentate subgranular zone and rostral subventricular zone after focal cerebral ischemia in the rat. Proc. Natl. Acad. Sci. USA *98*, 4710–4715. https://doi.org/10.1073/pnas.081011098.

Jin, X., Yu, Z.-F., Chen, F., Lu, G.-X., Ding, X.-Y., Xie, L.-J., and Sun, J.-T. (2017). Neuronal Nitric Oxide Synthase in Neural Stem Cells Induces Neuronal Fate Commitment via the Inhibition of Histone Deacetylase 2. Front. Cell. Neurosci. *11*, 66. https://doi.org/10.3389/fncel.2017.00066.

Kaneko, N., Herranz-Pérez, V., Otsuka, T., Sano, H., Ohno, N., Omata, T., Nguyen, H.B., Thai, T.Q., Nambu, A., Kawaguchi, Y., et al. (2018). New neurons use Slit-Robo signaling to migrate through the glial meshwork and approach a lesion for functional regeneration. Sci. Adv. *4*, eaav0618. https://doi.org/10.1126/sciadv.aav0618.

Lindvall, O., and Kokaia, Z. (2015). Neurogenesis following Stroke Affecting the Adult Brain. Cold Spring Harb. Perspect. Biol. *7*, a019034. https://doi.org/10.1101/cshperspect.a019034.

Luo, J., Shook, B.A., Daniels, S.B., and Conover, J.C. (2008). Subventricular zone-mediated ependyma repair in the adult mammalian brain. J. Neurosci. *28*, 3804–3813. https://doi.org/10.1523/JNEUROSCI.0224-08.2008.

Luzzati, F., Fasolo, A., and Peretto, P. (2011). Combining confocal laser scanning microscopy with serial section reconstruction in the study of adult neurogenesis. Front. Neurosci. *5*, 70. https://doi.org/10.3389/fnins.2011.00070.

Luzzati, F., Nato, G., Oboti, L., Vigna, E., Rolando, C., Armentano, M., Bonfanti, L., Fasolo, A., and Peretto, P. (2014). Quiescent neuronal progenitors are activated in the juvenile guinea pig lateral striatum and give rise to transient neurons. Development *141*, 4065–4075. https://doi.org/10.1242/dev.107987.

Madison, R.D., Zomorodi, A., and Robinson, G.A. (2000). Netrin-1 and Peripheral Nerve Regeneration in the Adult Rat. Exp. Neurol. *161*, 563–570. https://doi.org/10.1006/exnr.1999.7292.

Magnusson, J.P., Göritz, C., Tatarishvili, J., Dias, D.O., Smith, E.M.K., Lindvall, O., Kokaia, Z., and Frisén, J. (2014). A latent neurogenic program in astrocytes regulated by Notch signaling in the mouse. Science *346*, 237–241. https://doi.org/10.1126/science.346.6206.237.

Manda, K., Kavanagh, J.N., Buttler, D., Prise, K.M., and Hildebrandt, G. (2014). Low dose effects of ionizing radiation on normal tissue stem cells. Mutat. Res. Rev. Mutat. Res. *761*, 6–14. https://doi.org/10.1016/j.mrrev.2014.02.003.

De Marchis, S., Fasolo, A., and Puche, A.C. (2004). Subventricular zone-derived neuronal progenitors migrate into the subcortical forebrain to postnatal mice. J. Comp. Neurol. *476*, 290–300. https://doi.org/10.1002/cne.20217.

Masuda, T., Isobe, Y., Aihara, N., Furuyama, F., Misumi, S., Kim, T.S., Nishino, H., and Hida, H. (2007). Increase in neurogenesis and neuroblast migration after a small intracerebral hemorrhage in rats. Neurosci. Lett. *425*, 114–119. https://doi.org/10.1016/j.neulet.2007.08.039.

Merkle, F.T., Mirzadeh, Z., Alvarez-Buylla, A., FT, M., Z, M., and A, A.-B. (2007). Mosaic organization of neural stem cells in the adult brain. Science *317*, 381–384. https://doi.org/10.1126/science.1144914.

Mimura-Yamamoto, Y., Shinohara, H., Kashiwagi, T., Sato, T., Shioda, S., and Seki, T. (2017). Dynamics and function of CXCR4 in formation of the granule cell layer during hippocampal development. Sci. Rep. *7*, 5647. https://doi.org/10.1038/s41598-017-05738-7.

Mruthyunjaya, S., Manchanda, R., Godbole, R., Pujari, R., Shiras, A., and Shastry, P. (2010). Laminin-1 induces neurite outgrowth in human mesenchymal stem cells in serum/differentiation factors-free conditions through activation of FAK–MEK/ERK signaling pathways. Biochem. Biophys. Res. Commun. *391*, 43–48. https://doi.org/10.1016/j.bbrc.2009.10.158.

Nato, G., Caramello, a., Trova, S., Avataneo, V., Rolando, C., Taylor, V., Buffo, a., Peretto, P., and Luzzati, F. (2015). Striatal astrocytes produce neuroblasts in an excitotoxic model of Huntington's

disease. Development *142*, 840–845. https://doi.org/10.1242/dev.116657.

Ng, T., Ryu, J.R., Sohn, J.H., Tan, T., Song, H., Ming, G.L., and Goh, E.L.K. (2013). Class 3 Semaphorin Mediates Dendrite Growth in Adult Newborn Neurons through Cdk5/FAK Pathway. PLoS One *8*, e65572. https://doi.org/10.1371/journal.pone.0065572.

Nguyen, L.D., and Ehrlich, B.E. (2020). Cellular mechanisms and treatments for chemobrain: insight from aging and neurodegenerative diseases. EMBO Mol. Med. *12*, e12075. https://doi.org/10.15252/emmm.202012075.

O'Connor, C., Mullally, R.E., McComish, S.F., O'Sullivan, J., Woods, I., Schoen, I., Garre, M., Caldwell, M.A., Dervan, A., and O'Brien, F.J. (2025). Neurotrophic extracellular matrix proteins promote neuronal and iPSC astrocyte progenitor cell- and nanoscale process extension for neural repair applications. J. Anat. *246*, 585–601. https://doi.org/10.1111/joa.14163.

Ohab, J.J., Fleming, S., Blesch, A., and Carmichael, S.T. (2006). A Neurovascular Niche for Neurogenesis after Stroke. J. Neurosci. *26*, 13007–13016. https://doi.org/10.1523/JNEUROSCI.4323-06.2006.

Parent, J.M., Vexler, Z.S., Gong, C., Derugin, N., and Ferriero, D.M. (2002). Rat forebrain neurogenesis and striatal neuron replacement after focal stroke. Ann. Neurol. *52*, 802–813. https://doi.org/10.1002/ana.10393.

Piccirillo, S.G., Spiteri, I., Sottoriva, A., Touloumis, A., Ber, S., Price, S.J., Heywood, R., Francis, N.J., Howarth, K.D., Collins, V.P., et al. (2015). Contributions to drug resistance in glioblastoma derived from malignant cells in the sub-ependymal zone. Cancer Res. *75*, 194–202. https://doi.org/10.1158/0008-5472.CAN-13-3131.

Reese, N.D., and Schiller, G.J. (2013). High-dose cytarabine (HD araC) in the treatment of leukemias: A review. Curr. Hematol. Malig. Rep. *8*, 141–148. https://doi.org/10.1007/s11899-013-0156-3.

Reider-Groswasser, I.I., Groswasser, Z., Ommaya, A.K., Schwab, K., Pridgen, A., Brown, H.R., Cole, R., and Salazar, A.M. (2002). Quantitive imaging in late traumatic brain injury. Part I: late imaging parameters in closed and penetrating head injuries. Brain Inj. *16*, 517–525. https://doi.org/10.1080/02699050110119141.

Ren, X., Boriero, D., Chaiswing, L., Bondada, S., St. Clair, D.K., and Butterfield, D.A. (2019). Plausible biochemical mechanisms of chemotherapy-induced cognitive impairment ("chemobrain"), a condition that significantly impairs the quality of life of many cancer survivors. Biochim. Biophys. Acta. Mol. Basis Dis. *1865*, 1088–1097. https://doi.org/10.1016/j.bbadis.2019.02.007.

Rice, A.C., Khaldi, A., Harvey, H.B., Salman, N.J., White, F., Fillmore, H., and Bullock, M.R. (2003). Proliferation and neuronal differentiation of mitotically active cells following traumatic brain injury. Exp. Neurol. *183*, 406–417. https://doi.org/10.1016/S0014-4886(03)00241-3.

Shook, B.A., Lennington, J.B., Acabchuk, R.L., Halling, M., Sun, Y., Peters, J., Wu, Q., Mahajan, A., Fellows, D.W., and Conover, J.C. (2014). Ventriculomegaly associated with ependymal gliosis and declines in barrier integrity in the aging human and mouse brain. Aging Cell *13*, 340–350. https://doi.org/10.1111/acel.12184.

Sundholm-Peters, N.L., Yang, H.K.C., Goings, G.E., Walker, A.S., and Szele, F.G. (2004). Radial glia-like cells at the base of the lateral ventricles in adult mice. J. Neurocytol. *33*, 153–164. https://doi.org/10.1023/B:NEUR.0000029654.70632.3a.

Todd, K.L., Brighton, T., Norton, E.S., Schick, S., Elkins, W., Pletnikova, O., Fortinsky, R.H., Troncoso, J.C., Molfese, P.J., Resnick, S.M., et al. (2017). Ventricular and Periventricular Anomalies in the Aging and Cognitively Impaired Brain. Front. Aging Neurosci. *9*, 445. https://doi.org/10.3389/fnagi.2017.00445.

El Waly, B., Bertet, C., Paris, M., Falque, M., Milpied, P., Magalon, K., Cayre, M., and Durbec, P. (2022). Neuroblasts contribute to oligodendrocytes generation upon demyelination in the adult mouse brain. iScience *25*, 105102. https://doi.org/10.1016/j.isci.2022.105102.

Wang, L.L., Serrano, C., Zhong, X., Ma, S., Zou, Y., and Zhang, C.L. (2021). Revisiting astrocyte to neuron conversion with lineage tracing in vivo. Cell *184*, 5465–5481.e16. https://doi.org/10.1016/j.cell.2021.09.005.

Wang, S., Qiu, D., So, K.-F., Wu, E.X., Leung, L.H.T., Gu, J., and Khong, P.-L. (2013). Radiation induced brain injury: assessment of white matter tracts in a pre-clinical animal model using diffusion tensor MR imaging. J. Neuro Oncol. *112*, 9–15. https://doi.org/10.1007/s11060-012-1031-0.

Wardill, H.R., Mander, K.A., Van Sebille, Y.Z.A., Gibson, R.J., Logan, R.M., Bowen, J.M., and Sonis, S.T. (2016). Cytokine-mediated blood brain barrier disruption as a conduit for cancer/chemotherapy-associated neurotoxicity and cognitive dysfunction. Int. J. Cancer *139*, 2635–2645. https://doi.org/10.1002/ijc.30252.

Was, H., Borkowska, A., Bagues, A., Tu, L., Liu, J.Y.H., Lu, Z., Rudd, J.A., Nurgali, K., and Abalo, R. (2022). Mechanisms of Chemotherapy-Induced Neurotoxicity. Front. Pharmacol. *13*, 750507. https://doi.org/10.3389/fphar.2022.750507.

Williamson, M.R., Le, S.P., Franzen, R.L., Donlan, N.A., Rosow, J.L., Nicot-Cartsonis, M.S., Cervantes, A., Deneen, B., Dunn, A.K., Jones, T.A., and Drew, M.R. (2023). Subventricular zone cytogenesis provides trophic support for neural repair in a mouse model of stroke. Nat. Commun. *14*, 6341. https://doi.org/10.1038/s41467-023-42138-0.

Winocur, G., Vardy, J., Binns, M.A., Kerr, L., and Tannock, I. (2006). The effects of the anti-cancer drugs, methotrexate and 5-fluorouracil, on cognitive function in mice. Pharmacol. Biochem. Behav. *85*, 66–75. https://doi.org/10.1016/j.pbb.2006.07.010.

Yamashita, T., Ninomiya, M., Herna, P., Garcı, J.M., Sunabori, T., Sakaguchi, M., Adachi, K., Kojima, T., Hirota, Y., Kawase, T., et al. (2006). Subventricular Zone-Derived Neuroblasts Migrate and Differentiate into Mature Neurons in the Post-Stroke Adult Striatum. J Neurosci. *26*, 6627–6636. https://doi.org/10.1523/JNEUROSCI.0149-06.2006.

Yang, Y., Estrada, E.Y., Thompson, J.F., Liu, W., and Rosenberg, G.A. (2007). Matrix Metalloproteinase-Mediated Disruption of Tight Junction Proteins in Cerebral Vessels is Reversed by Synthetic Matrix Metalloproteinase Inhibitor in Focal Ischemia in Rat. J. Cereb. Blood Flow Metab. *27*, 697–709. https://doi.org/10.1038/sj.jcbfm.9600375.

Young, C.C., Brooks, K.J., Buchan, A.M., and Szele, F.G. (2011). Cellular and molecular determinants of stroke-induced changes

in subventricular zone cell migration. Antioxid. Redox Signal. *14*, 1877–1888. https://doi.org/10.1089/ars.2010.3435.

Zamboni, M., Llorens-Bobadilla, E., Magnusson, J.P., and Frisén, J. (2020). A Widespread Neurogenic Potential of Neocortical Astrocytes Is Induced by Injury. Cell Stem Cell *27*, 605–617.e5. https://doi.org/10.1016/j.stem.2020.07.006.

Zhang, W., Xiao, D., Mao, Q., and Xia, H. (2023). Role of neuroinflammation in neurodegeneration development. Signal Transduct. Target. Ther. *8*, 267. https://doi.org/10.1038/s41392-023-01486-5.

Zhang, Y., Li, B., Cananzi, S., Han, C., Wang, L.-L., Zou, Y., Fu, Y.-X., Hon, G.C., and Zhang, C.-L. (2022). A single factor elicits multilineage reprogramming of astrocytes in the adult mouse striatum. Proc. Natl. Acad. Sci. USA *119*, e2107339119. https://doi.org/10.1073/pnas.2107339119.

Zhao, M., Momma, S., Delfani, K., Carlén, M., Cassidy, R.M., Johansson, C.B., Brismar, H., Shupliakov, O., Frisén, J., and Janson, A.M. (2003). Evidence for neurogenesis in the adult mammalian substantia nigra. Proc. Natl. Acad. Sci. USA *100*, 7925–7930. https://doi.org/10.1073/pnas.1131955100.